# Development of New Cyclic Plasmin Inhibitors with Excellent Potency and Selectivity

Sebastian M. Saupe, Stephanie Leubner, Michael Betz, Gerhard Klebe, and Torsten Steinmetzer*

Department of Pharmacy, Institute of Pharmaceutical Chemistry, Philipps University Marburg, Marbacher Weg 6, D-35032 Marburg, Germany

S *Supporting Information*

ABSTRACT: The trypsin-like serine protease plasmin is a target for the development of antifibrinolytic drugs for use in cardiac surgery with cardiopulmonary bypass or organ transplantations to reduce excessive blood loss. The optimization of our recently described substrate-analogue plasmin inhibitors, which were cyclized between their P3 and P2 side chains, provided a new series with improved efficacy and excellent selectivity. The most potent inhibitor **8** binds to plasmin with an inhibition constant of 0.2 nM, whereas K_i values >1 μM were determined for nearly all other tested trypsin-like serine proteases, with the exception of trypsin, which is also inhibited in the nanomolar range. Docking studies revealed a potential binding mode in the widely open active site of plasmin that explains the strong potency and selectivity profile of these inhibitors. The dialkylated piperazine-linker segment contributes to an excellent solubility of all analogues. Based on their overall profile the presented inhibitors are well suited for further development as injectable antifibrinolytic drugs.
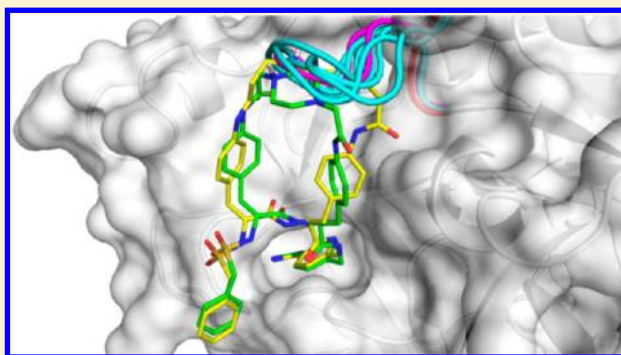
INTRODUCTION

The ubiquitously expressed trypsin-like serine protease plasmin is responsible for the dissolution of fibrin clots in blood, where it is normally regulated by their endogenous inhibitors α_2-antiplasmin and α_2-macroglobulin. Its zymogen plasminogen is primarily released from the liver into the circulation and becomes mainly activated by the plasminogen activator tPA, whereas uPA is responsible for the generation of plasmin in the intercellular space.[1,2] Beyond its fibrinolytic function, plasmin cleaves and activates many other substrates including metalloproteases, growth factors, and extracellular matrix proteins, thereby mediating cell migration, which enables normal physiological processes, like embryogenesis, wound healing, and angiogenesis. Otherwise, plasmin also promotes tumor progression and metastasis, as well as chronic inflammatory processes.[3,4] Inhibitors of plasmin can be clinically used for the treatment of hyperfibrinolysis, which may occur during cardiac surgery with cardiopulmonary bypass or organ transplantations.[5,6] Additional applications could be the treatment of heavy menstrual bleeding[7] or some forms of hemophilia. A beneficial effect of plasmin inhibitors has been also proposed for the treatment of rare forms of hereditary angioedema[8,9] and certain lymphoid malignancies[10,11] or chronic inflammatory processes.[4]

For many years, the 58 amino acid long Kunitz-type serine protease inhibitor aprotinin[12] was clinically used for the reduction of perioperative bleeding.[13] Due to later reported side effects, it was withdrawn from the market in 2008,[14,15] but was reintroduced in Canada in 2011.[16] Meanwhile, aprotinin

was mainly replaced by the lysine analog tranexamic acid and in a few cases also by ε-aminocaproic acid. Both compounds inhibit the activation of plasminogen but have no direct inhibitory effect on active plasmin. In contrast to aprotinin, tranexamic acid has to be administered in relatively high doses, which has been linked to convulsive seizures.[17,18] It was proposed that high dose tranexamic acid induces hyperexcitability and convulsions due to blocking γ-aminobutyric acid-driven inhibition of the central nervous system.[19] Therefore, the development of new and safe plasmin inhibitors as replacement for aprotinin, especially for use in cardiac surgery, is of high interest.

Only a few potent plasmin inhibitors have yet been reported in literature.[20] Among them are tetrapeptide derivatives containing a C-terminal arginal group,[21] derivatives of *trans*-4-aminomethylcyclohexanecarboxylic acid,[22,23] and cyclic ketone-based inhibitors.[24,25]

A series of highly potent plasmin inhibitors was derived from substrate analogue structures containing a C-terminal 4-amidinobenzylamide residue.[26] One of these derivatives, CU-2010 (structure not yet disclosed), inhibits plasmin with a K_i value of 2.2 nM[27] and has reached clinical development to reduce blood loss in cardiac surgery. It was recently reported that its further development was stopped in phase 2b due to serious side effects, although no further information has been

Scheme 1. Structures of Recently Described Cyclic Plasmin Inhibitors[32]
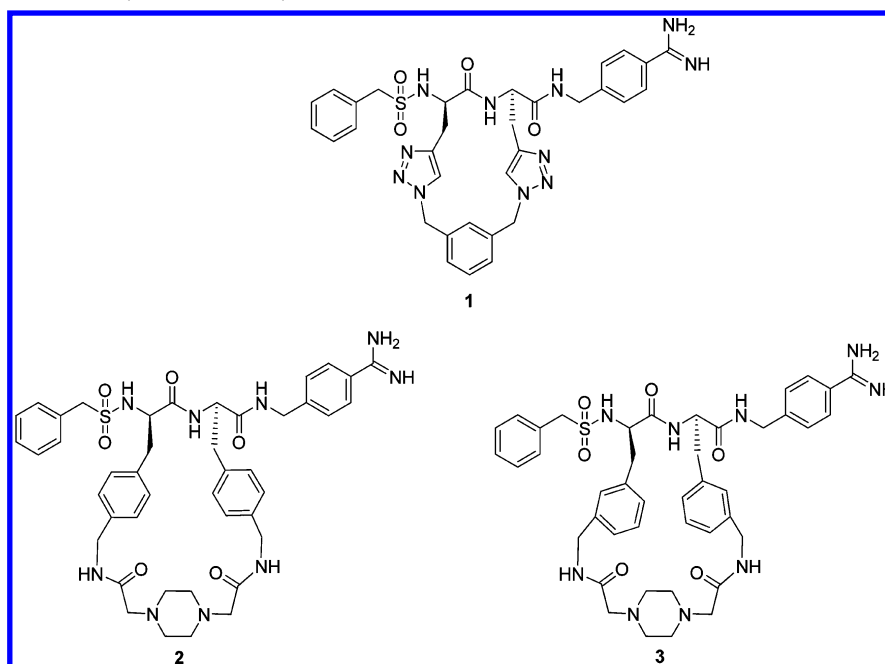
announced for the exact problems that occurred.[28] It should be noted that CU-2010 has only limited selectivity and also inhibits plasma kallikrein, factor Xa, and factor XIa in the nanomolar range,[27] which could be a potential disadvantage, as discussed recently.[20] Although there exist many examples for approved nonselective drugs, for example, in the field of kinase inhibitors,[29] a high target selectivity is normally a primary objective in drug development.[30] However, the design of selective substrate analogue inhibitors for the approximately 70 different trypsin-like serine proteases is a challenging task. All of them have a similar S1 pocket and enable recognition of substrate analogue structures by highly conserved backbone interactions to the P1 and P3 residues.[31]

Starting from linear substrate-analogue 4-amidinobenzylamide derivatives, we have recently reported a structure-based development of cyclized plasmin inhibitors with significantly improved selectivity.[32] The cyclization was performed between the side chains of the D-configured P3 and L-configured P2 amino acids via amide bond couplings, metathesis, or click chemistry. The most potent analog **1** (Scheme 1) of this series inhibits plasmin and plasma kallikrein (PK) with K_i values of 0.8 and 2.4 nM, respectively, whereas it has negligible activity against the related proteases thrombin, factor Xa (fXa), and activated protein C (aPC). Molecular modeling revealed that the rigid cyclic ring structure of compound **1** prevents its binding to thrombin, factor Xa, and activated protein C due to a steric repulsion from an active site loop next to the amino acid residue 99 (chymotrypsinogen numbering) present in these proteases. In contrast, the ring segment of inhibitor **1** fits well into the widely open active site of plasmin, which is missing this 99-loop. The deletion of the segment 95−100 is a unique structural feature of plasmin that results in a direct connection of residue 94 to amino acid 101, which is named as 94-shunt.[33] PK contains a glycine in position 99 resulting in a sterically less crowded 99-loop, which therefore still allows an unperturbed binding of inhibitor **1**.

Despite its excellent potency against plasmin and PK, inhibitor **1** suffers from two drawbacks. For use as an injectable

drug, it possesses only a limited solubility of approximately 0.2 mg/mL in 0.9% saline. In addition, its synthesis requires the preparation of the potentially hazardous intermediate 1,3-bis(azidomethyl)benzene, which was used for the ring closure reaction under microwave conditions. Better soluble analogues of this first series, like **2** and **3** containing a bis-alkylated piperazine linker, suffered from reduced potency and selectivity.[32]
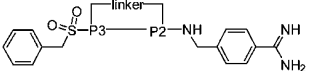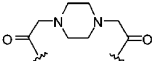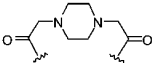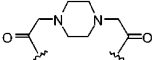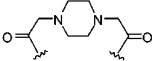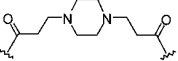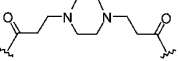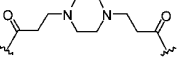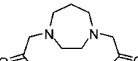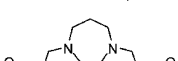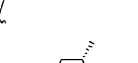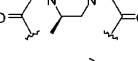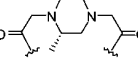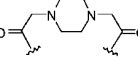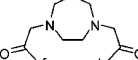
Therefore, a new series of well-soluble cyclized plasmin inhibitors was developed. All analogues were tested against a panel of related trypsin-like serine proteases, and it was found that some of the most potent inhibitors possess an excellent selectivity for plasmin. The modeled binding mode of these analogues in the active site of plasmin reveals an explanation for their high specificity compared with other trypsin-like serine proteases. In this paper, we describe the synthesis and characterization of these new analogues.

RESULTS

Synthesis. Many studies with related inhibitors of various trypsin-like serine proteases, like thrombin,[34,35] factor Xa,[36,37] factor VIIa,[38,39] and uPA,[40] emphasized the important contribution of the P1 amidinobenzylamide and P4 benzylsulfonyl group for a high inhibitory potency. Therefore, both anchor residues were maintained, and we have focused only on the optimization of the cyclic ring structure. A bis-alkylated piperazine derivative was generally used for connecting the P3 and P2 residues, which contributes to an excellent solubility of all inhibitors. Replacement of the various amidomethylenephenylalanines in P3 and P2 position of inhibitors **2** and **3** by the shorter amidophenylalanine residues provided analogs **4−14**, which differ only in the position of the amide group on the P2 and P3 phenyl rings and the used bis-alkylated piperazine segment (Table 1).

Scheme 2 summarizes the synthesis strategy for the preparation of inhibitors **4** and **8**. The synthesis started from H-D-Phe(NO$_2$)-OH, which was treated with benzylsulfonyl chloride. Intermediate **18** was coupled with commercially

Table 1. Structures of the Synthesized Cyclic Inhibitors

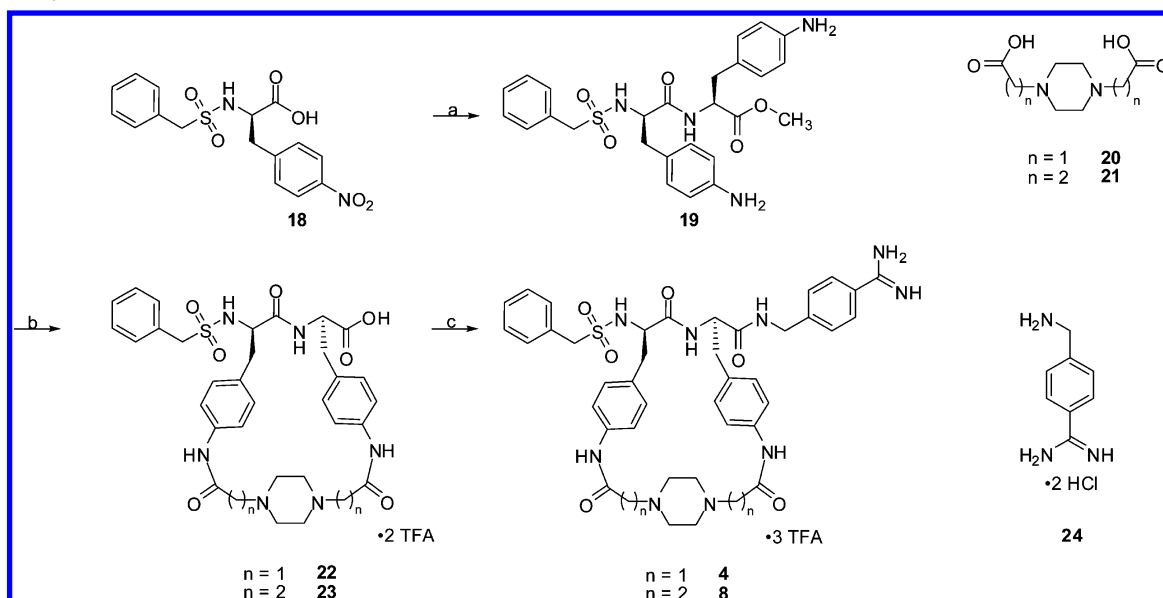| Inhibitor	P3	P2	Linker	plasmin	PK	thrombin	fXa	aPC	trypsin[b]
1[a]				0.77	2.4	9490	206	3000	580
2[a]		Structures are provided in scheme 1.		9.0	493	3517	3472	3510	9.4
3[a]				4.1	25	7.2	21	48	1.0
4	D-Phe(4-NH-)	Phe(4-NH-)		0.68	320	13870	>10000	>25000	62.6
5	D-Phe(3-NH-)	Phe(3-NH-)		7.0	3.2	227	12.3	39	3.4
6	D-Phe(4-NH-)	Phe(3-NH-)		25	12.9	8017	1803	4100	19.4
7	D-Phe(3-NH-)	Phe(4-NH-)		9.0	118	604	415	420	7.8
8	D-Phe(4-NH-)	Phe(4-NH-)		0.20	1000	26420	25000	>15000	38.3
9	D-Phe(4-NH-)	Phe(3-NH-)		5.1	24.0	3250	237	880	24.9
10	D-Phe(3-NH-)	Phe(4-NH-)		4.0	240	376	1260	3800	0.6
11	D-Phe(4-NH-)	Phe(4-NH-)		0.57	392	14143	7357	>10000	3.0
12	D-Phe(4-NH-)	Phe(4-NH-)		1.32	422	11210	8500	7800	10.2
13[c]	D-Phe(4-NH-)	Phe(4-NH-)		1.15	500	12082	14042	>20000	18.1
14	D-Phe(4-NH-)	Phe(4-NH-)		1.62	242	8510	3700	4800	55.0
15	D-Phe(4-CH2-NH-)	Phe(4-NH-)		0.52	187	884	2510	3900	17.8
16	D-Phe(4-CH2-NH-)	Phe(4-NH-)		0.76	440	5870	9000	>10000	41.7
17	D-Phe(4-CH2-NH-)	Phe(4-NH-)		1.71	116	2950	3250	1600	126

[a]These compounds have been previously published; their K_i values are provided as reference.[32] [b]Porcine trypsin; all other enzymes are from human source (see Supporting Information). [c]Due to the incorporation of the *trans*-2,5-dimethylpiperazine, this compound should exist in two configuration isomers; however, only a single peak was observed for the final inhibitor in HPLC.

available H-Phe(NO$_2$)-OMe, followed by reduction of both nitro groups, for example, by treatment with zinc dust in 90% acetic acid. Alternatively, this reduction could also be performed with similar yields by hydrogenation using Pd/C as catalyst in 90% acetic acid or by transfer hydrogenation using ammonium formate.[41] The obtained bis-amine **19** was cyclized with the piperazine derivatives **20** or **21**, followed by saponification of the methyl ester. The obtained intermediates

22 and **23** were coupled with 4-amidinobenzylamine·2HCl (**24**)[42] yielding inhibitors **4** and **8**.

Inhibitors **15**−**17** (Table 1) were prepared as exemplarily described for compound **15** in Scheme 3. All analogs contain a D-4-amidomethylenephenylalanyl group in P3 position, a 4-amidophenylalanyl as P2 residue but differ in the used piperazine linker. The synthesis started from intermediate **25**,[32] which was coupled to commercially available H-Phe(NH$_2$)-OMe, followed by removal of the Cbz protection

Scheme 2. Synthesis of Inhibitors 4 and 8[a]

[a](a) (i) 1 equiv of **18**, 1 equiv of H-Phe(4-NO$_2$)-OMe·HCl, 1 equiv of PyBOP, 2 equiv of DIPEA, DMF, 0 °C; (ii) zinc powder, 90% AcOH, room temp, preparative HPLC, 80% yield (two steps); (b) (i) 1 equiv of **19**, 1 equiv of **20** or **21**, 2 equiv of PyBOP, 4 equiv of DIPEA, DMF, 2 h 0 °C, room temp overnight; (ii) 1 N NaOH, EtOH/water, room temp, preparative HPLC, 17.9% yield (**22**), 12.0% yield (**23**) (two steps); (c) 1 equiv of **22** or **23**, 3 equiv of NMM, 1 equiv of isobutyl chloroformate, DMF, −15 °C, 10 min, followed by 1.5 equiv of **24** and 1 equiv of NMM, 1 h at −15 °C, room temp overnight, preparative HPLC, 32.9% yield (**4**), 38.3% yield (**8**).

Scheme 3. Synthesis of Inhibitor 15[a]
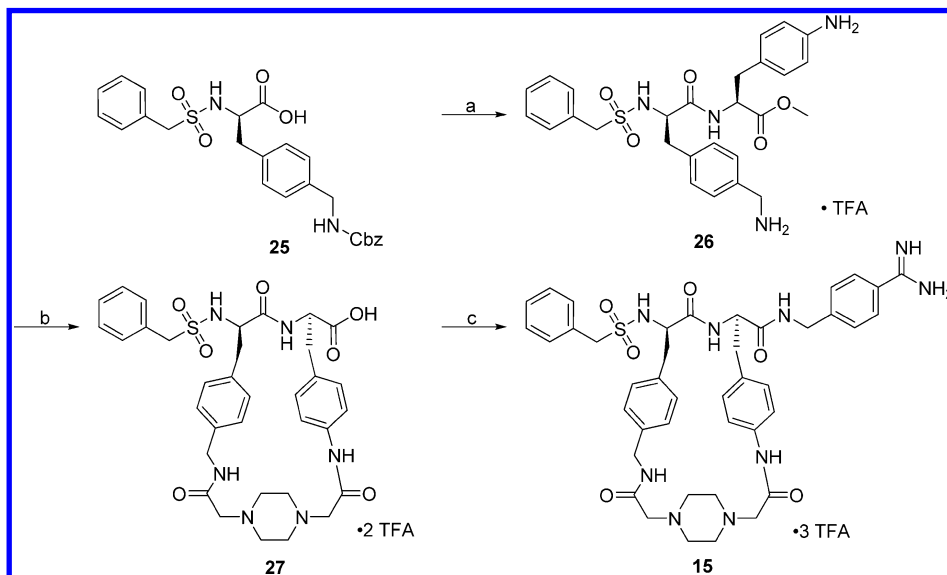
[a](a) (i) 1 equiv of **25**, 1 equiv of H-Phe(4-NH$_2$)-OMe·HCl, 1 equiv of PyBOP, 2 equiv of DIPEA, DMF, 0 °C; (ii) 32% HBr in acetic acid, precipitation by diethyl ether, preparative HPLC, 30.5% yield (two steps); (b) (i) 1 equiv of **26**, 1 equiv of **20**, 2 equiv of PyBOP, 5 equiv of DIPEA, DMF, 0 °C; (ii) 1 N NaOH, EtOH/water, room temp, preparative HPLC, 29.6% yield (two steps); (c) 1 equiv of **27**, 3 equiv of NMM, 1 equiv of isobutyl chloroformate, DMF, −15 °C, 10 min, followed by 1.5 equiv of **24** and 1 equiv of NMM, 1 h at −15 °C, room temp overnight, preparative HPLC 32.8% yield.

with 32% HBr in acetic acid. The following steps were performed as described above in Scheme 2. The intermediate **26** was cyclized with the appropriate piperazine derivatives, followed by saponification and coupling of 4-amidinobenzyla-mine·2HCl.

The piperazine dicarbonic acids **20** and **21**, and the *trans*-2,5-dimethylpiperazine diacetic acid (see Supporting Information) were obtained by alkylation of the appropriate piperazine

derivatives with bromoacetic or 3-bromopropionic acid under basic conditions. After acidification with concentrated HCl, the products precipitated and could be isolated by filtration, as described previously.[43,44] Surprisingly, no precipitation occurred after the analogous alkylation of the homopiperazine and *cis*-2,5-dimethylpiperazine[45] with bromoacetic acid, followed by acidification. This prohibited a simple purification of these very hydrophilic intermediates and required a more

laborious synthesis of these dialkylated piperazine analogs. In that case, benzyl or *tert*-butyl bromoacetate was used for the alkylation of these piperazine derivatives resulting in more hydrophobic intermediates, which could be purified by reversed phase HPLC. Hydrogenation of the benzyl ester or acidic cleavage of the *tert*-butyl ester provided the appropriate products, which were isolated by precipitation in diethyl ether (see Supporting Information).

Kinetic Measurements. The inhibition constants of all newly synthesized inhibitors **4−17** are summarized in Table 1. The K_i values for compounds **1−3** from our first series[32] are provided as reference (Table 1).

Inhibitor **4**, a direct analog of compound **2** missing two methylene spacer groups in the ring structure, was found to be an excellent plasmin inhibitor with a K_i of 0.68 nM. It exhibits further improved selectivity compared with compound **1**, which was also a strong inhibitor of PK and retained some affinity for fXa. In contrast, all of these newly prepared compounds inhibit trypsin more strongly than analog **1**. However, although trypsin was used as an additional reference enzyme in our study, it is not a relevant protease in blood. The analogous inhibitors **5−7** contain the identical diacetyl-piperazine linker but differ in the position of the amide substitution on both phenyl groups in the P2 and P3 residues. These three analogs had reduced selectivity and potency against plasmin suggesting that we should maintain the amide substitution in *para* position at both phenyl rings.

The incorporation of the longer dipropionyl-piperazine in inhibitor **8** further improved the affinity against plasmin and retained the excellent selectivity. Also in that case the *para* amide substitution on the P2 and P3 phenyl rings is preferred, both analogues **9** and **10** have reduced selectivity and potency as plasmin inhibitors. The diacetyl-homopiperazine inhibitor **11** has a very similar inhibition profile, as found for its direct analogue **4**, whereas the dipropionyl-homopiperazine **12** has reduced potency compared with the piperazine derivative **8**. No benefit was observed after incorporation of the *trans*- and *cis*-2,5-dimethyl-piperazine linker in inhibitors **13** and **14**. Analogs **15−17** contain an amidomethylene substitution in *para* position of the P3 phenyl ring. Inhibitors **15** and **16** have a comparable inhibitory potency against plasmin as found for their direct analogs **4** and **11**, but a marginally reduced selectivity. The incorporation of the *cis*-2,5-dimethyl-piperazine in inhibitor **17** provided no advantage, similar to what was already observed for compound **14**.

Further Characterization of Inhibitors 4 and 8. The detected inhibitory profile revealed that several derivatives of the current series are excellent and highly selective plasmin inhibitors. Among several suitable candidates the chemically well-accessible compounds **4** and **8** were selected for extended selectivity studies with additional trypsin-like serine proteases (Table 2). Both inhibitors possess a negligible affinity against most of the other proteases confirming the hypothesis that the rigid cyclic inhibitor structure might be repelled by their 99-loop. However, both analogues inhibit human trypsin slightly more strongly than the porcine enzyme used for the data shown in Table 1.

Additional tests were performed with compounds **4** and **8** (Table 3), which possess the most suitable overall profile (data provided by the Medicines Company Leipzig GmbH, whereby the assays were performed as described previously).[46] Due to the piperazine linker, the inhibitors possess an excellent solubility in 0.9% saline, which is a prerequisite for an injectable

Table 2. Extended Selectivity Studies with Inhibitors 4 and 8

	K_i (nM)[a]	
protease	inhibitor **4**	inhibitor **8**
urinary kallikrein	>50000	ca. 10000
human C1s	>100000	>35000
human C1r	>50000	>35000
human FXIa	4700	3370
human FXIIa	>100000	>20000
human FVIIa/TF	>30000	>50000
human FIXa	>100000	>5000
human tPA	>100000	>40000
human uPA	8900	ca. 6500
human trypsin	44	8.4

[a]Data provided by the Medicines Company Leipzig GmbH.

Table 3. Further Characterization of Inhibitors 4 and 8[a]

	inhibitor **4**	inhibitor **8**
thermodynamic solubility in 0.9% saline [mg/mL]	>2	>2
tPA-induced fibrinolysis in human plasma: EC$_{200}$ for clot-to-lysis time [nM][b]	280	180
plasma clotting times in human plasma (EC$_{200}$) [μM][b]		
(a) PT	>100	>100
(b) aPTT	>100	>100
(c) TT	>100	>100
hERG [% binding at 10 μM][c]	7	4
Na channel [% binding at 10 μM][c]	−8	27
L-type Ca channels [% binding at 10 μM][c]		
(a) benzothiazepine	1	−4
(b) dihydropyridine	−2	−5
(c) phenylalkylamine	13	3
human plasma protein binding [% free fraction]	61	67
stability in human liver microsomes [% degradation in 60 min]	0	2
CYP-450 inhibition, IC$_{50}$ [μM][c]		
3A4	>22	>10
2D6	>40	>10
2C9	>100	>100
1A2	>100	>100
2C19	>10	>100

[a]Data provided by the Medicines Company Leipzig GmbH. [b]The assays were described previously.[46] [c]Assays were performed at MDS Pharma services, Taipei; the used protocols are provided in the Supporting Information (negative values reveal no binding).

drug. Both compounds efficiently inhibit the tPA-induced fibrinolysis in human plasma.[46] The necessary concentrations for the doubling of the clot to lysis time (EC$_{200}$)[46] are 280 nM for inhibitor **4** and 180 nM for compound **8**. Due to their negligible inhibitory effect on the corresponding clotting proteases, both inhibitors showed no anticoagulant activity in plasma. EC$_{200}$ values >100 μM were determined for the doubling of clotting times in the thrombin time (TT), activated partial thromboplastin time (aPTT), and prothrombin time (PT) assays.[46] At a concentration of 10 μM both compounds showed no significant binding to the tested hERG, natrium, and L-type calcium ion channels (these assays were performed at MDS Pharma services, Taipei, Taiwan, now Ricerca Biosciences; the used protocols are provided in the Supporting Information). A 60 min incubation with human liver microsomes revealed negligible metabolization of both compounds.
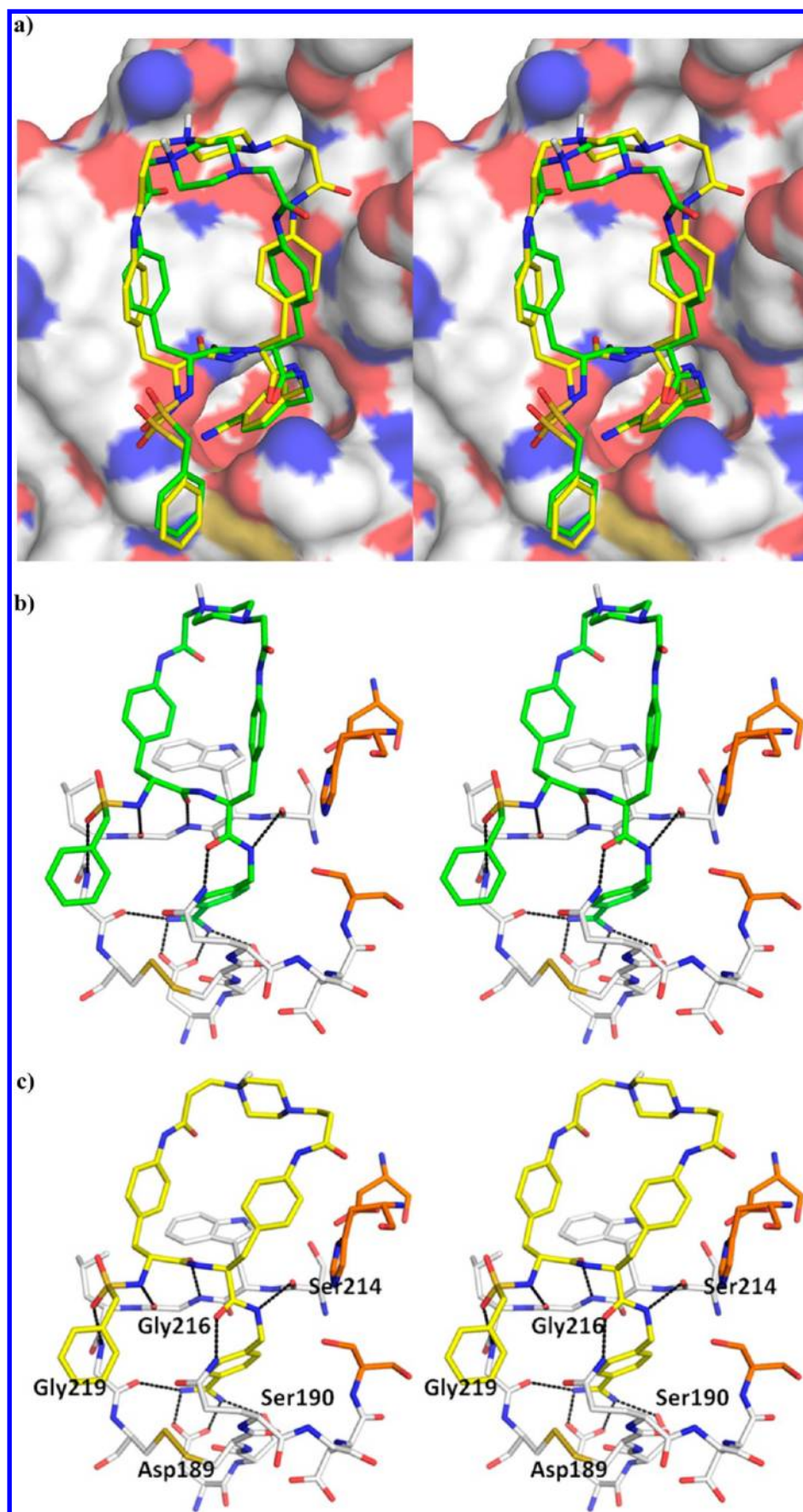
Figure 1. Stereoview of the modeled binding modes of inhibitors **4** (with green carbon atoms) and **8** (yellow carbon atoms) in plasmin (PDB code 1bui); the coordinate files are provided in pdb format in the Supporting Information.[33] Both inhibitors are shown in their singly protonated form at

F

dx.doi.org/10.1021/jm3012917 | J. Med. Chem. XXXX, XXX, XXX−XXX

Figure 1. continued

the piperazine moiety; the position of the protonation is indicated. (a) Overlay of both inhibitor structures in the active site of plasmin, shown with its solvent-accessible surface color-coded by atom types (carbon in white, oxygen red, nitrogen blue, sulfur yellow). The overall binding mode reveals that the larger macrocycle of inhibitor **8** binds closer to the plasmin surface. (b) Stereoview of inhibitor **4** in plasmin showing potential hydrogen bonds. The residues of the catalytic triad, shown with orange carbon atoms, are not involved in any interaction with the inhibitor. (c) Analogous stereoview of inhibitor **8** in plasmin; the residues involved in hydrogen bonds to the inhibitor are labeled.[51]
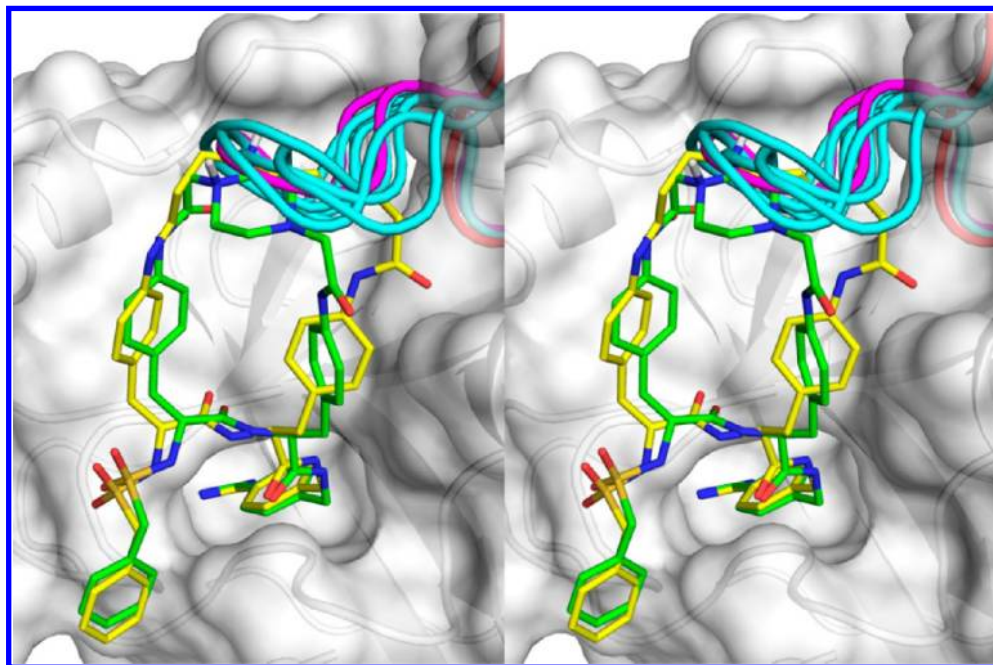

Figure 2. Stereoview of the modeled structure of inhibitors **4** (with green carbon atoms) and **8** (yellow carbons) in complex with plasmin (PDB code 1bui). The protein is shown with its translucent solvent-accessible surface in gray. The plasmin backbone is also colored in gray, whereby its segment Arg94-Lys101-Asp102 is provided as red tube in the upper right corner. These plasmin−inhibitor complexes were overlaid with the crystal structures of aPC (1aut), fXa (2pr3), PK (2any), and thrombin (1k22), whereby of these proteases only their backbones between residues 94 and 102 are indicated as turquoise tubes. In these orientations, the loops will induce a major sterical clash with the macrocyclic ring structures of both inhibitors and supposedly prohibit their proper binding. The analogous loop of trypsin (2ra3) is shown in magenta and located at a very similar position.

All IC$_{50}$ values for the inhibition of various cytochrome P450 enzymes were found to be >10 μM.

Docking of Inhibitors 4 and 8 in Plasmin. Inhibitors **4** and **8** were docked into the active site of plasmin using FlexX considering different protonation states of the piperazine moiety in the linker segment. In previous experimental studies with N,N′-bisalkylated piperazine derivatives, like N,N′-piperazine-dicarbonic acid,[47] N,N′-piperazine-diacetic acid,[48] and N,N′-dimethylpiperazine,[49] it was found that only one of the nitrogens is protonated at physiological pH. Additional pK_a calculations with 3,3′-(piperazine-1,4-diyl)bis(N-phenylpropanamide), which is identical to the linker segment of inhibitor **8**, were performed with the Marvin Suite[50] and also provided a singly protonated piperazine as major microspecies at physiological pH 7.4 and also at pH 8.0, as used for the kinetic measurements (calculated pK_a values of 8.54 and 3.01 for the nitrogens). In contrast, an unprotonated piperazine was obtained as major microspecies for the shorter 2,2′-(piperazine-1,4-diyl)bis(N-phenylacetamide), which is part of the linker in inhibitor **4** (calculated pK_a values 6.08 and 0.58). Due to the uncertainty of the piperazine protonation, three possibilities were considered for docking. In the first case, both nitrogens were unprotonated, whereas in the second and

third case only one of them was protonated. The unlikely double protonated form was omitted.

The docked structures shown in Figure 1 contain a singly protonated piperazine moiety in the macrocycle and were selected based on similar backbone interactions known from related complexes of noncyclized substrate analogue inhibitors, for example, with thrombin, factor Xa, factor VIIa, trypsin, or urokinase. In addition, we have also obtained very similar inhibitor conformations for analogs with unprotonated macrocycles. Identical hydrogen bonds were found in both complexes. The P1-amidino group forms the characteristic salt bridge to Asp189 and hydrogen bonds to the carbonyl group of Gly219 and the side chain oxygen of Ser190, whereas the amide NH of the P1 residue binds to the carbonyl oxygen of Ser214. A H-bond is also suggested between the P2 carbonyl oxygen of both inhibitors and the side chain amide of Gln192 (2.4 and 2.5 Å). In addition, the typical antiparallel β-sheet interaction between Gly216 and the P3 backbone can be found, and one sulfonyl oxygen is involved in a hydrogen bond to the NH of Gly219. The comparison of both inhibitor conformations reveals that the longer and therefore more flexible cycle of inhibitor **8** adapts better to the plasmin surface allowing for stronger van der Waals contacts, whereby the piperazine linker segment of analog **4** is directed more toward the solvent.

However, we could not detect any specific hydrogen bond between the linker segment and plasmin.

The generated docking solutions of both inhibitors in plasmin were also overlaid with crystal structures of PK, thrombin, fXa, aPC, and trypsin. In Figure 2, plasmin is shown with its transparent solvent-accessible surface in gray and its specific 94-shunt as red tube. From the other proteases only their loop segment 94−102 is shown as tube colored in turquoise (PK, thrombin, fXa, aPC) or magenta (trypsin). These segments protrude from the plasmin surface, because this loop is completely missing in plasmin. Following this model, a sterical clash between these loops and the piperazine portion of the ligand's macrocycle should be generated, which serves as a reasonable explanation for the observed excellent selectivity profile against most of the trypsin-like serine proteases. However, an exception is trypsin; although it contains a very similar 99 loop, it is still potently inhibited by this type of macrocyclic inhibitor.

■ DISCUSSION

The results from enzyme kinetic analysis with these new derivatives supports our previous hypothesis that it is possible to develop selective substrate analog plasmin inhibitors by appropriate macrocyclization between the side chains of a P2 amino acid in the L-configuration and a D-configured P3 residue. The newly developed cyclization variant, introduced into inhibitors 4 and 8, starts directly with an amide substitution in the *para* position of the P2 and P3 phenyl rings and provides convenient chemical access to highly potent plasmin inhibitors. They exhibit an improved selectivity profile compared with our first series, particularly a reduced affinity against PK.[32] Although a beneficial anti-inflammatory effect of aprotinin during cardiac surgery due to its PK inhibitory activity (K_i 30 nM) was described in several publications,[52,53] there are also controversial reports that an inhibition of the kallikrein−kinin system leads to a loss of the protective effects of kinins against ischemia-reperfusion injury.[54] This is considered to be one of the reasons for the increased number of myocardial infarction and stroke after application of aprotinin, which does not achieve satisfactory selectivity discrimination between plasmin and PK. Locally increased bradykinin levels, which would be the consequence of a reduced PK inhibition, result in an increased coronary blood flow, and have been reported to play a beneficial role in cardiac diseases.[55] Based on this concept, inhibitors of the lysosomal serine carboxypeptidase cathepsin A, a degrading protease of bradykinin, have been very recently described for the potential treatment of cardiovascular diseases.[56] Despite controversial results regarding the effects of differences in the bradykinin levels due to variations in the enzymatic activity of bradykinin generating and degrading proteases, a high specificity of a drug should generally minimize undesired side effects. A molecular scaffold with convincing discriminative power between similar proteases should be an advantage for further development.

Another major advantage of the new macrocyclic inhibitors is their straightforward chemical accessibility. The synthesis of these compounds does not require any hazardous azide intermediates, reactions under drastic microwave conditions, or application of special and costly catalysts, which are necessary for click chemistry and metathesis reaction steps during the preparation of our previous series. However, the yield-limiting cyclization step still requires further optimization. Several small scale reactions using intermediate 19 revealed that

the cyclization performs slightly better using the shorter diacetyl-piperazine 20 compared with the coupling of the longer analog 21.

The modeled structures of inhibitors 4 and 8 in plasmin provide a plausible binding mode explaining their high affinity. All known interactions of the P1 4-amidinobenzylamide at the bottom of the S1 pocket and to the carbonyl oxygen of Ser214 at the entrance of this binding site can be accomplished. The stronger affinity of inhibitor 8 compared with 4 might be explained by more extensive van der Waals contacts of the macrocyclic ring structure, which is oriented slightly closer toward the plasmin surface. The modeled complexes of inhibitors 4 and 8 in plasmin, superimposed with the X-ray structures of the other proteases, reveal a sterical clash with their active site loops around the amino acid 99 explaining the observed selectivity profile. An exception is trypsin, which is still significantly inhibited by both compounds. The digestive protease trypsin is mainly located in the intestinal tract and normally should not come in direct contact with an injectable plasmin inhibitor, although minor levels of trypsinogen and trypsin have been detected also in other organs, in body fluids, or in cancer cells, especially in pancreatitis patients.[57] Clinical studies with the thrombin inhibitor melagatran,[58] which also inhibits trypsin with a K_i value of 4 nM,[59] revealed that an inhibitory potency against trypsin is obviously no disadvantage for an injectable drug. It should be noted that the trypsin used for the inhibition studies shown in Table 2 is isolated from human pancreas (Calbiochem, CAS 9002-07-7, PN 650275-50UG), and this material is not only one single protein. Native trypsin consists of a mixture of approximately two-thirds cationic trypsin (trypsin-1), one-third anionic trypsin (trypsin-2), and a few percent of mesotrypsin (trypsin-3), including isoforms.[57] However, human trypsin-1, -2, and -3 contain a normal loop between their residues 94−100 with leucine in position 99 and without any amino acid deletion, which consists of the sequences YDRKTLN, YNSRTLD, and YNRDTLD, respectively. At present, we can only speculate that the 99-loop in trypsin is more flexible than those in other proteases and still enables a significant binding of inhibitors 4 and 8, although both compounds are more than 40-fold stronger plasmin inhibitors. A higher flexibility of the 99-loop could be also the reason that trypsin is a relatively nonselective protease degrading most substrates as long as they contain a basic P1 residue. However, the comparison of several crystal structures of trypsin-like serine proteases, which were used in our selectivity studies, did not reveal higher B-factors for the 99-loop of trypsin (see Figure S1 in the Supporting Information). Admittedly, the analysis of the B-factors of individual crystal structures is certainly not a sufficient criterion to characterize the loop flexibility in proteins.

In conclusion, we could develop a series of new cyclic plasmin inhibitors and have found an excellent overall profile for inhibitors 4 and 8. In addition to their strong inhibitory potency on plasmin and high selectivity over related trypsin-like serine proteases, both compounds possess a strong anti-fibrinolytic activity in plasma, excellent solubility, and a low affinity to the tested ion channels and cytochrome P450 enzymes. These properties should justify their further characterization in animal models for the treatment of pathological conditions associated with increased plasmin activities, especially for the reduction of blood loss during cardiac surgery or as antidote during thrombolytic therapy.

■ EXPERIMENTAL SECTION

General. Reagents and solvents were purchased from Aldrich Chemical, Acros Organics, Alfa Aesar, Fluka, Iris Biotech, PepTech, or Polypeptide. The amino acid derivatives H-Phe(4-NO$_2$)-OH, H-D-Phe(4-NO$_2$)-OH, and H-Phe(4-NH$_2$)-OH were purchased from PepTech and Bachem.

Analytical HPLC experiments were performed on a Shimadzu LC-10A system (column, NUCLEODUR C$_{18}$ ec, 5 μm, 100 Å, 4.6 mm × 250 mm, Machery-Nagel, Düren, Germany). As eluents were used water (A) and acetonitrile (B) both containing 0.1% TFA at a flow rate of 1 mL/min, a linear gradient (1% B/min) and detection at 220 nm. The indicated purity for all intermediates is based on HPLC detection at 220 nm. The final inhibitors were purified to >95% purity (detection at 220 nm) by preparative HPLC (pumps, Varian PrepStar model 218 gradient system; detector, ProStar model 320; fraction collector, Varian model 701) using a C$_{18}$ column (ProntoSIL C18 SH, 5 μm, 120 Å, 32 mm × 250 mm, Bischoff Chromatography) and a linear gradient of acetonitrile/water containing 0.1% TFA at a flow rate of 20 mL/min. All inhibitors were finally obtained as TFA salts after lyophilization. The molecular mass of the synthesized compounds was determined using a QTrap 2000 ESI spectrometer (Applied Biosystems). The ^{1}H and ^{13}C NMR spectra were recorded on an ECX-400 instrument (Jeol Inc.) and are referenced to internal solvent signals.

Bzls-D-Phe(4-NO$_2$)-OH (18). H-D-Phe(4-NO$_2$)-OH (4.93 g, 23.5 mmol, 1.0 equiv) was suspended in 56 mL of dry DCM and treated with TMS-Cl (6.5 mL, 52.4 mmol, 2.2 equiv) and DIPEA (9.1 mL, 52.4 mmol, 2.2 equiv). The mixture was refluxed for 1 h. Then, benzylsulfonyl chloride (5.02 g, 26.3 mmol, 1.1 equiv) was added in several portions within 35 min at 0 °C, and the pH was maintained at 8−9 by addition of DIPEA (4.6 mL, 26.2 mmol, 1.1 equiv). The mixture was stirred for 1 h at 0 °C and 2 h at room temperature. The solvent was removed in vacuo, and the brown residue was dissolved in a mixture of 5% KHSO$_4$ and EtOAc. The solution was extracted twice with EtOAc. The combined organic phase was washed thrice with 5% KHSO$_4$ and thrice with brine. The organic layer was dried over MgSO$_4$ and filtered, and the solvent was removed in vacuo.

The remaining residue was dissolved in 250 mL of ethyl acetate and dropwise treated with dicyclohexylamine (7.14 mL, 35.7 mmol, 1.5 equiv). The dicyclohexylammonium salt crystallized at 4 °C and was isolated by filtration. The crystals were washed with EtOAc and diethylether and were dried in vacuo (yield, 7.94 g (62.1%) of beige DCHA-salt crystals).

The dicyclohexylammonium salt (2.70 g, 4.95 mmol) was dissolved in a mixture of 5% KHSO$_4$/EtOAc, and the water phase was extracted thrice with EtOAc. The combined organic phases were washed once with brine, dried over MgSO$_4$, and filtered. The solvent was evaporated. Yield: 1.80 g (99.8%) of brown oil. HPLC: 38.7 min, start at 10% B (purity, 95.3%). ^{1}H NMR (400 MHz, DMSO-d_6): δ = 12.97 (br. s., 1 H), 8.15 (d, J = 8.70 Hz, 2 H), 7.70 (d, J = 8.70 Hz, 1 H), 7.51 (d, J = 8.70 Hz, 2 H), 7.12−7.31 (m, 5 H), 4.10−4.20 (m, 2 H), 4.04−4.10 (m, 1 H), 3.11 (dd, J = 5.50, 13.74 Hz, 1 H), 2.93 ppm (dd, J = 9.16, 13.74 Hz, 1 H). ^{13}C NMR (101 MHz, DMSO-d_6): δ = 172.7, 146.4, 145.5, 130.9, 130.7, 130.0, 128.1, 127.9, 123.2, 58.5, 56.8, 37.5 ppm. MS (ESI, positive): calcd, 364.07; m/z, 382.17 [M + NH$_4$]$^+$, 387.06 [M+Na]$^+$.

Bzls-D-Phe(4-NH$_2$)-Phe(4-NH$_2$)-OMe (19). Compound **18** (1.80 g, 4.94 mmol, 1.0 equiv) and H-Phe(4-NO$_2$)-OMe·HCl (1.29 g, 4.95 mmol, 1.0 equiv) were dissolved in 30 mL of DMF and stirred on an ice bath. After 10 min, PyBOP (2.60 g, 5.00 mmol, 1.0 equiv) and DIPEA (1.72 mL, 9.89 mmol, 2.0 equiv) were added, and the mixture was stirred for 1 h at 0 °C and 2 h at room temperature, pH 7−8. The solvent was removed in vacuo, and the remaining residue was dissolved in a mixture of 5% KHSO$_4$ and EtOAc. The organic phase was washed thrice with 5% KHSO$_4$, once with brine, thrice with saturated aqueous NaHCO$_3$, and thrice with brine. The organic phase was dried over MgSO$_4$ and filtered, and the solvent was removed in vacuo. Yield, 3.55 g of a brown solid containing impurity. HPLC: 51.8

min, start at 10% B (purity, 88.7%). MS (ESI, positive): calcd, 570.57; m/z, 571.23 [M + H]$^+$.

The intermediate (3.5 g, approximately 4.87 mmol, 1.0 equiv) was dissolved in 500 mL of 90% AcOH, and after addition of zinc dust (2.6 g, 39.8 mmol, 8.0 equiv), the suspension was stirred for 5 h. After filtration, the solvent was evaporated. The remaining residue was suspended in 50 mL of 90% MeCN, the precipitated zinc acetate was removed by centrifugation, and the supernatant was evaporated. The remaining residue was purified by preparative HPLC and lyophilized from 80% *tert*-butanol/water. Yield: 2.02 g (80.0%) of a yellow lyophilized solid. HPLC: 17.4 min, start at 10% B (purity, 93.5%). ^{1}H NMR (400 MHz, DMSO-d_6): δ = 8.68 (d, J = 7.79 Hz, 1 H), 7.53 (d, J = 9.16 Hz, 1 H), 7.22−7.31 (m, 4 H), 7.18 (dd, J = 3.66, 7.33 Hz, 2 H), 7.14 (d, J = 4.35 Hz, 2 H), 7.12 (s, 1 H), 6.99 (d, J = 8.47 Hz, 2 H), 6.90 (d, J = 8.24 Hz, 2 H), 4.46 (dt, J = 5.72, 8.24 Hz, 2 H), 4.09 (dt, J = 4.47, 9.45 Hz, 2 H), 3.90 (dd, J = 13.50, 53.00 Hz, 4 H), 3.53−3.58 (m, 3 H), 2.97 (dd, J = 5.30, 13.70 Hz, 1 H), 2.81 (dd, J = 9.16, 13.74 Hz, 1 H), 2.63 (dd, J = 4.60, 13.70 Hz, 1 H), 2.54 ppm (dd, J = 9.85, 13.51 Hz, 1 H). ^{13}C NMR (101 MHz, DMSO-d_6): δ = 171.7, 171.1, 158.8, 158.5, 134.9, 134.7, 133.7, 130.7, 130.3, 130.0, 128.2, 127.9, 121.0, 120.6, 58.5, 57.8, 53.5, 52.0, 37.9, 36.2 ppm. MS (ESI, positive): calcd, 510.61; m/z, 511.27 [M + H]$^+$.

2,2′-(Piperazine-1,4-diyl)diacetic Acid (20). The synthesis was performed as described previously.[43]

3,3′-(Piperazine-1,4-diyl)dipropanoic Acid (21). Piperazine·6-H$_2$O (5.0 g, 25.7 mmol, 1.0 equiv) was dissolved in 140 mL of 10% NaOH, treated with 3-bromopropionic acid (8.08 g, 52.8 mmol, 2.05 equiv) and stirred overnight at room temperature. The mixture was acidified with 37% HCl until the product started to crystallize. The flask was kept at 4 °C overnight, and the product was obtained by filtration, washed with a small amount of water, and dried in vacuo. Yield: 4.58 g (77.4%) of light yellow crystals. ^{1}H NMR (400 MHz, D$_2$O): δ = 3.71 (br. s, 8 H), 3.56 (t, J = 6.87 Hz, 4 H), 2.90 ppm (t, J = 6.90 Hz, 4 H). ^{13}C NMR (101 MHz, D$_2$O): δ = 173.3, 52.2, 48.6, 28.4 ppm. MS (ESI, negative): calcd, 230.13; m/z, 229.17 [M − H]$^-$.

Compound 22. Bzls-D-Phe(4-NH$_2$)-Phe(4-NH$_2$)-OMe (**19**) (201 mg, 0.394 mmol, 1.0 equiv) and 2,2′-(piperazine-1,4-diyl)diacetic acid (**20**) (79.8 mg, 0.395 mmol, 1.0 equiv) were dissolved in 200 mL of DMF and stirred on an ice bath. After 10 min, PyBOP (410.8 mg, 0.789 mmol, 2.0 equiv) and DIPEA (409 μL, 2.35 mmol, 6.0 equiv) were added, and the mixture was stirred at pH 8 for 1 h at 0 °C and at room temperature overnight. The solvent was removed in vacuo, and the remaining residue was dissolved in a mixture of saturated aqueous NaHCO$_3$ and EtOAc. The organic layer was washed thrice with saturated aqueous NaHCO$_3$ and thrice with a small amount of brine, dried over MgSO$_4$, and filtered, and the solvent was evaporated. The remaining residue was dissolved in 5.0 mL of 50% 1 N NaOH/ethanol (v/v). The solution was stirred for 2 h at room temperature and neutralized with TFA, and the solvent was removed in vacuo. The residue was purified by preparative HPLC and lyophilized. Yield: 63 mg (17.9%) of a white lyophilized solid. HPLC: 22.6 min, start at 10% B (purity, >95%). ^{1}H NMR (400 MHz, DMSO-d_6): δ = 12.75−13.07 (m, 1 H), 9.99−10.40 (m, 2 H), 8.68 (br. s., 1 H), 6.81−7.78 (m, 13 H), 6.43−6.79 (m, 2 H), 4.12−4.59 (m, 5 H), 2.60−3.75 ppm (m, 16 H). ^{13}C NMR (101 MHz, DMSO-d_6): δ = 173.1, 170.3, 158.9, 158.6, 136.5, 131.0, 130.4, 129.5, 129.2, 128.3, 128.0, 119.6, 119.2, 118.1, 67.0, 58.5, 56.1, 54.0, 48.9, 31.3 ppm. MS (ESI, positive): calcd, 662.76; m/z, 663.35 [M + H]$^+$.

Compound 23. According to the synthesis of compound **22**, Bzls-D-Phe(4-NH$_2$)-Phe(4-NH$_2$)-OMe (**19**) (200 mg, 0.392 mmol, 1.0 equiv), 3,3′-(piperazine-1,4-diyl)dipropanoic acid (**21**) (90.1 mg, 0.391 mmol, 1.0 equiv), PyBOP (409 mg, 0.786 mmol, 2.0 equiv), and DIPEA (273 μL, 1.57 mmol, 4.0 equiv) were cyclized in 120 mL of DMF, followed by saponification in 5.0 mL of 50% 1 N NaOH/ethanol (v/v) for 3 h at room temperature. The solution was neutralized with TFA, and the solvent was removed in vacuo. The residue was purified by preparative HPLC and lyophilized. Yield: 43 mg (12.0%) of a white lyophilized solid. HPLC: 22.5 min, start at 10% B (purity, 90.8%). ^{1}H NMR (400 MHz, DMSO-d_6): δ = 12.81−13.17 (m, 1 H), 9.93 (br. s., 2 H), 8.60 (d, J = 6.41 Hz, 1 H), 6.62−7.68 (m,

13 H), 6.48 (br. s., 2 H), 3.80–4.53 (m, 9 H), 2.55–3.57 ppm (m, 16 H). ^{13}C NMR (101 MHz, DMSO-d_6): δ = 172.7, 169.5, 169.0, 168.9, 158.6, 158.3, 137.3, 137.0, 130.8, 130.2, 130.1, 129.8, 128.3, 128.0, 119.9, 119.7, 67.0, 58.0, 56.5, 53.9, 48.9, 36.1, 31.3 ppm. MS (ESI, positive): calcd, 690.28; m/z, 691.24 $[M + H]^+$.

4-Amidinobenzylamine·2HCl (24). The synthesis was performed as described previously.[42]

Inhibitor 4. Compound **22** (54 mg, 69.5 μmol, 1.0 equiv) and NMM (23.0 μL, 209 μmol, 3.0 equiv) were dissolved in 1.5 mL of DMF at −15 °C and treated with isobutyl chloroformate (9.0 μL, 69.5 μmol, 1.0 equiv). The mixture was stirred for 10 min at −15 °C and treated with 4-amidinobenzylamine·2HCl (24 mg, 108 μmol, 1.6 equiv) and NMM (7.7 μL, 69.5 μmol, 1.0 equiv). The suspension was stirred at −15 °C for 1 h and at room temperature overnight. The solvent was removed in vacuo; the product was purified by preparative HPLC and lyophilized. Yield: 26 mg (32.9%) of a white lyophilized solid. HPLC: 18.1 min, start at 10% B (purity, > 95%).

^{1}H NMR (400 MHz, DMSO-d_6): δ = 10.19 (br. s, 2 H), 9.22 (br. s., 2 H), 9.12 (br. s., 2 H), 8.73 (br. s., 2 H), 7.59–7.81 (m, 3 H), 6.74–7.58 (m, 17 H), 3.94–4.73 (m, 10 H), 2.62–3.32 ppm (m, 12 H). MS (ESI, positive): calcd, 793.34; m/z 794.51 $[M + H]^+$. TLC: R_f = 0.28.

Inhibitor 8. The synthesis was performed as described for inhibitor **4**. The mixed anhydride was prepared from compound **23** (35 mg, 38.1 μmol, 1.0 equiv), NMM (12.6 μL, 114 μmol, 3.0 equiv), and isobutyl chloroformate (5.0 μL, 38.1 μmol, 1.0 equiv) in 1.5 mL of DMF at −15 °C. After 10 min, compound **24** (13 mg, 58.5 μmol, 1.5 equiv) and NMM (4.2 μL, 38.1 μmol, 1.0 equiv) were added; the mixture was stirred 1 h at −15 °C and at room temperature overnight. The product was purified by preparative HPLC and lyophilized. Yield: 17 mg (38.3%) of a white lyophilized solid. HPLC: 19.8 min, start at 10% B (purity, > 95%). ^{1}H NMR (400 MHz, DMSO-d_6): δ = 9.83–10.01 (m, 2 H), 9.19 (s, 2 H), 8.91 (br. s., 2 H), 8.75–8.82 (m, 1 H), 8.63 (d, J = 7.33 Hz, 1 H), 7.67 (d, J = 8.24 Hz, 2 H), 7.34–7.49 (m, 4 H), 7.20–7.28 (m, 5 H), 7.08 (s, 4 H), 6.41–6.57 (m, 2 H), 6.33 (br. s., 2 H), 4.33–4.60 (m, 8 H), 4.28 (s, 2 H), 4.18 (s, 1 H), 2.62–3.18 ppm (m, 16 H). MS (ESI, positive): calcd, 821.37; m/z, 822.33 $[M + H]^+$, 411.61 $[M + 2H]^{2+}$. TLC: R_f = 0.10.

Enzyme Kinetics. The kinetic measurements with human plasmin (Chromogenix; spec. activity = 13.6 casein units/mg, concentration in assay of 0.895 nM) were performed in a microplate reader (Multiscan Ascent, Thermo) at 405 nm using the substrate Tos-Gly-Pro-Lys-pNA (Chromozym PL, concentrations in assay of 364, 182, and 91 μM). The K_i values were determined from Dixon plots.[60] The inhibition constants for the reference enzymes PK, thrombin, FXa, and aPC were performed as described previously (see Supporting Information).[61]

Molecular Modeling. *Preparation of Plasmin.* The coordinates of the protease domain of plasmin taken from the microplasmin−staphylokinase−microplasmin ternary complex irreversibly inhibited by H-Glu-Gly-Arg-chloromethyl ketone (PDB code 1bui) were used for docking. All water molecules and covalent bonds of the inhibitor to plasmin residues His57 and Ser195 were removed. Protonation of the plasmin's binding site was performed by use of the receptor preparation tool of FlexX.[62]

Inhibitor Preparation and Docking. Ligands **4** and **8** were prepared using the MOE[63] builder function, whereby three different protonation states of the piperazine linker have been considered. In the first case, both nitrogens are unprotonated, and in the second and third cases only one of them is protonated. For the docking process, various conformers of the macrocycle were generated using the conformational search procedures of MOE (conformational search using LowModeMD,[64] stochastically, and systematically search; all other standard parameters were set to default values). This search provided a library of 87 and 275 conformers for the macrocycles of inhibitors **4** and **8**, respectively, which were used for docking with FlexX. These pregenerated macrocycles were treated as rigid objects during docking.

The active site of plasmin was defined by taking all residues within a 16 Å sphere around the center of mass of the inhibitor in the crystal structure. Two interactions between the ligand and the carbonyl oxygens of Ser214 and Gly216 were set as essential docking restraints.

In addition, two optional interactions were set to the side chain of Asp189, whereby one has to be addressed and the second is optional. The best ranked poses were subsequently minimized using the MMFF94x force field implemented in MOE.

ASSOCIATED CONTENT

Ⓢ Supporting Information

It contains the synthesis procedures for all other inhibitors, their analytical data, and information for enzyme kinetics and the coordinate files of the modeled complexes of inhibitors **4** and **8** in plasmin in pdb format. This material is available free of charge via the Internet at http://pubs.acs.org.

AUTHOR INFORMATION

Corresponding Author

*Phone: +49 6421 2825900. E-mail: steinmetzer@staff.uni-marburg.de.

Notes

The authors declare no competing financial interest.

ACKNOWLEDGMENTS

ABBREVIATIONS USED

AMe, aminomethyl; Boc, *tert*-butyloxycarbonyl; Bzls, benzyl-sulfonyl; Cbz, benzyloxycarbonyl; DIPEA, *N,N*-diisopropyle-thylamine; DCHA, dicyclohexylamine; DCM, dichlorome-thane; DMF, *N,N*-dimethylformamide; EtOAc, ethyl acetate; Me, methyl; MeCN, acetonitrile; MS, mass spectrometry; NMM, 4-methylmorpholine; Phe(4-AMe), 4-aminomethylphe-nylalanine; Phe(4-NH$_2$), 4-aminophenylalanine; Phe(4-NO$_2$), 4-nitrophenylalanine; PK, plasma kallikrein; PN, product number; PyBOP, benzotriazol-1-yl-oxytripyrrolidinophospho-nium hexafluorophosphate; tBu, *tert*-butyl; TFA, trifluoroacetic acid; TMS-Cl, trimethylsilyl chloride

REFERENCES

(1) Vassalli, J. D.; Sappino, A. P.; Belin, D. The plasminogen activator/plasmin system. *J. Clin. Invest.* **1991**, *88*, 1067−1072.

(2) Schaller, J.; Gerber, S. S. The plasmin-antiplasmin system: Structural and functional aspects. *Cell. Mol. Life Sci.* **2011**, *68*, 785−801.

(3) Castellino, F. J.; Ploplis, V. A. Structure and function of the plasminogen/plasmin system. *Thromb. Haemostasis* **2005**, *93*, 647−654.

(4) Syrovets, T.; Lunov, O.; Simmet, T. Plasmin as a proin-flammatory cell activator. *J. Leukocyte Biol.* **2012**, *92*, 509−519.

(5) Levy, J. H. Pharmacologic methods to reduce perioperative bleeding. *Transfusion* **2008**, *48*, 31S−38S.

(6) Johansson, P. I.; Ostrowski, S. R.; Secher, N. H. Management of major blood loss: An update. *Acta Anaesthesiol. Scand.* **2010**, *54*, 1039−1049.

(7) Philipp, C. S. Antifibrinolytics in women with menorrhagia. *Thromb. Res.* **2011**, *127* (Suppl 3), S113−115.

(8) Ritchie, B. C. Protease inhibitors in the treatment of hereditary angioedema. *Transfus. Apheresis Sci.* **2003**, *29*, 259−267.

(9) Du-Thanh, A.; Raison-Peyron, N.; Drouet, C.; Guillot, B. Efficacy of tranexamic acid in sporadic idiopathic bradykinin angioedema. *Allergy* **2010**, *65*, 793−795.

(10) Okada, Y.; Tsuda, Y.; Wanaka, K.; Tada, M.; Okamoto, U.; Okamoto, S.; Hijikata-Okunomiya, A.; Bokonyi, G.; Szende, B.; Keri, G. Development of plasmin and plasma kallikrein selective inhibitors and their effect on M1 (melanoma) and HT29 cell lines. *Bioorg. Med. Chem. Lett.* **2000**, *10*, 2217−2221.

(11) Ishihara, M.; Nishida, C.; Tashiro, Y.; Gritli, I.; Rosenkvist, J.; Koizumi, M.; Okaji, Y.; Yamamoto, R.; Yagita, H.; Okumura, K.; Nishikori, M.; Wanaka, K.; Tsuda, Y.; Okada, Y.; Nakauchi, H.; Heissig, B.; Hattori, K. Plasmin inhibitor reduces T-cell lymphoid tumor growth by suppressing matrix metalloproteinase-9-dependent CD11b(+)/F4/80(+) myeloid cell recruitment. *Leukemia* **2012**, *26*, 332−339.

(12) Ascenzi, P.; Bocedi, A.; Bolognesi, M.; Spallarossa, A.; Coletta, M.; De Cristofaro, R.; Menegatti, E. The bovine basic pancreatic trypsin inhibitor (Kunitz inhibitor): A milestone protein. *Curr. Protein Pept. Sci.* **2003**, *4*, 231−251.

(13) Mannucci, P. M.; Levi, M. Prevention and treatment of major blood loss. *New Engl. J. Med.* **2007**, *356*, 2301−2311.

(14) Mangano, D. T.; Tudor, I. C.; Dietzel, C. The risk associated with aprotinin in cardiac surgery. *New Engl. J. Med.* **2006**, *354*, 353−365.

(15) Schneeweiss, S.; Seeger, J. D.; Landon, J.; Walker, A. M. Aprotinin during coronary-artery bypass grafting and risk of death. *New Engl. J. Med.* **2008**, *358*, 771−783.

(16) Sniecinski, R. M.; Karkouti, K.; Levy, J. H. Managing clotting: A North American perspective. *Curr. Opin. Anaesthesiol.* **2012**, *25*, 74−79.

(17) Murkin, J. M.; Falter, F.; Granton, J.; Young, B.; Burt, C.; Chu, M. High-dose tranexamic acid is associated with nonischemic clinical seizures in cardiac surgical patients. *Anesth. Analg.* **2010**, *110*, 350−353.

(18) Sander, M.; Spies, C. D.; Martiny, V.; Rosenthal, C.; Wernecke, K.-D.; von Heymann, C. Mortality associated with administration of high-dose tranexamic acid and aprotinin in primary open-heart procedures: a retrospective analysis. *Crit. Care* **2010**, *14*, R148.

(19) Furtmueller, R.; Schlag, M. G.; Berger, M.; Hopf, R.; Huck, S.; Sieghart, W.; Redl, H. Tranexamic acid, a widely used antifibrinolytic agent, causes convulsions by a gamma-aminobutyric acid(A) receptor antagonist effect. *J. Pharmacol. Exp. Ther.* **2002**, *301*, 168−173.

(20) Swedberg, J. E.; Harris, J. M. Natural and engineered plasmin inhibitors: Applications and design strategies. *ChemBioChem* **2012**, *13*, 336−348.

(21) Swedberg, J. E.; Harris, J. M. Plasmin substrate binding site cooperativity guides the design of potent peptide aldehyde inhibitors. *Biochemistry* **2011**, *50*, 8454−8462.

(22) Okada, Y.; Tsuda, Y.; Tada, M.; Wanaka, K.; Okamoto, U.; Hijikata-Okunomiya, A.; Okamoto, S. Development of potent and selective plasmin and plasma kallikrein inhibitors and studies on the structure-activity relationship. *Chem. Pharm. Bull.* **2000**, *48*, 1964−1972.

(23) Tsuda, Y.; Tada, M.; Wanaka, K.; Okamoto, U.; Hijikata-Okunomiya, A.; Okamoto, S.; Okad, Y. Structure-inhibitory activity relationship of plasmin and plasma kallikrein inhibitors. *Chem. Pharm. Bull.* **2001**, *49*, 1457−1463.

(24) Xue, F.; Seto, C. T. Selective inhibitors of the serine protease plasmin: probing the S3 and S3′ subsites using a combinatorial library. *J. Med. Chem.* **2005**, *48*, 6908−6917.

(25) Xue, F.; Seto, C. T. Structure-activity studies of cyclic ketone inhibitors of the serine protease plasmin: design, synthesis, and biological activity. *Bioorg. Med. Chem.* **2006**, *14*, 8467−8487.

(26) Steinmetzer, T.; Schweinitz, A.; Stuerzebecher, J.; Steinmetzer, P.; Soffing, A.; Van de Locht, A.; Nicklisch, S.; Reichelt, C.; Ludwig, F.-A.; Schulze, A.; Daghisch, M.; Heinicke, J. Trypsin-like serine protease inhibitors, and their preparation and use. U.S. Pat. Appl. 20100022781, 2010.

(27) Szabo, G.; Veres, G.; Radovits, T.; Haider, H.; Krieger, N.; Baehrle, S.; Miesel-Groeschel, C.; Niklisch, S.; Karck, M.; van de Locht, A. Effects of novel synthetic serine protease inhibitors on postoperative blood loss, coagulation parameters, and vascular relaxation after cardiac surgery. *J. Thorac. Cardiovasc. Surg.* **2010**, *139*, 181−188.

(28) Mitchell, M. The Medicines Company Discontinues Phase 2b Trial of MDCO-2010. http://ir.themedicinescompany.com/phoenix.zhtml?c=122204&p=irol-newsArticle&ID=1741990&highlight= (accessed 10-31-2012).

(29) Fabian, M. A.; Biggs, W. H., 3rd; Treiber, D. K.; Atteridge, C. E.; Azimioara, M. D.; Benedetti, M. G.; Carter, T. A.; Ciceri, P.; Edeen, P. T.; Floyd, M.; Ford, J. M.; Galvin, M.; Gerlach, J. L.; Grotzfeld, R. M.; Herrgard, S.; Insko, D. E.; Insko, M. A.; Lai, A. G.; Lelias, J. M.; Mehta, S. A.; Milanov, Z. V.; Velasco, A. M.; Wodicka, L. M.; Patel, H. K.; Zarrinkar, P. P.; Lockhart, D. J. A small molecule-kinase interaction map for clinical kinase inhibitors. *Nat. Biotechnol.* **2005**, *23*, 329−336.

(30) Huggins, D. J.; Sherman, W.; Tidor, B. Rational approaches to improving selectivity in drug design. *J. Med. Chem.* **2012**, *55*, 1424−1444.

(31) Perona, J. J.; Craik, C. S. Structural basis of substrate specificity in the serine proteases. *Protein Sci.* **1995**, *4*, 337−360.

(32) Saupe, S. M.; Steinmetzer, T. A new strategy for the development of highly potent and selective plasmin inhibitors. *J. Med. Chem.* **2012**, *55*, 1171−1180.

(33) Parry, M. A.; Fernandez-Catalan, C.; Bergner, A.; Huber, R.; Hopfner, K. P.; Schlott, B.; Gührs, K. H.; Bode, W. The ternary microplasmin-staphylokinase-microplasmin complex is a proteinase-cofactor-substrate complex in action. *Nat. Struct. Biol.* **1998**, *5*, 917−923.

(34) Tucker, T. J.; Lumma, W. C.; Mulichak, A. M.; Chen, Z.; Naylor-Olsen, A. M.; Lewis, S. D.; Lucas, R.; Freidinger, R. M.; Kuo, L. C. Design of highly potent noncovalent thrombin inhibitors that utilize a novel lipophilic binding pocket in the thrombin active site. *J. Med. Chem.* **1997**, *40*, 830−832.

(35) Wiley, M. R.; Chirgadze, N. Y.; Clawson, D. K.; Craft, T. J.; Gifford-Moore, D. S.; Jones, N. D.; Olkowski, J. L.; Weir, L. C.; Smith, G. F. D-Phe-Pro-p-amidinobenzylamine: A potent and highly selective thrombin inhibitor. *Bioorg. Med. Chem. Lett.* **1996**, *6*, 2387−2392.

(36) Stürzebecher, A.; Dönnecke, D.; Schweinitz, A.; Schuster, O.; Steinmetzer, P.; Stürzebecher, U.; Kotthaus, J.; Clement, B.; Stürzebecher, J.; Steinmetzer, T. Highly potent and selective substrate analogue factor Xa inhibitors containing D-homophenylalanine analogues as P3 residue: Part 2. *ChemMedChem* **2007**, *2*, 1043−1053.

(37) Dönnecke, D.; Schweinitz, A.; Stürzebecher, A.; Steinmetzer, P.; Schuster, M.; Stürzebecher, U.; Nicklisch, S.; Stürzebecher, J.; Steinmetzer, T. From selective substrate analogue factor Xa inhibitors to dual inhibitors of thrombin and factor Xa. Part 3. *Bioorg. Med. Chem. Lett.* **2007**, *17*, 3322−3329.

(38) Shiraishi, T.; Kadono, S.; Haramura, M.; Kodama, H.; Ono, Y.; Iikura, H.; Esaki, T.; Koga, T.; Hattori, K.; Watanabe, Y.; Sakamoto, A.; Yoshihashi, K.; Kitazawa, T.; Esaki, K.; Ohta, M.; Sato, H.; Kozono, T. Factor VIIa inhibitors: target hopping in the serine protease family using X-ray structure determination. *Bioorg. Med. Chem. Lett.* **2008**, *18*, 4533−4537.

(39) Kadono, S.; Sakamoto, A.; Kikuchi, Y.; Oh-eda, M.; Yabuta, N.; Yoshihashi, K.; Kitazawa, T.; Suzuki, T.; Koga, T.; Hattori, K.; Shiraishi, T.; Haramura, M.; Kodama, H.; Ono, Y.; Esaki, T.; Sato, H.; Watanabe, Y.; Itoh, S.; Ohta, M.; Kozono, T. Structure-based design of P3 moieties in the peptide mimetic factor VIIa inhibitor. *Biochem. Biophys. Res. Commun.* **2005**, *327*, 589−596.

(40) Schweinitz, A.; Steinmetzer, T.; Banke, I. J.; Arlt, M. J.; Stürzebecher, A.; Schuster, O.; Geissler, A.; Giersiefen, H.; Zeslawska, E.; Jacob, U.; Kruger, A.; Stürzebecher, J. Design of novel and selective inhibitors of urokinase-type plasminogen activator with improved pharmacokinetic properties for use as antimetastatic agents. *J. Biol. Chem.* **2004**, *279*, 33613−33622.

(41) Anwer, M. K.; Spatola, A. F. An advantageous method for the rapid removal of hydrogenolyzable protecting groups under ambient conditions; synthesis of leucine-enkephalin. *Synthesis* **1980**, 929–932.

(42) Becker, G. L.; Sielaff, F.; Than, M. E.; Lindberg, I.; Routhier, S.; Day, R.; Lu, Y.; Garten, W.; Steinmetzer, T. Potent inhibitors of furin and furin-like proprotein convertases containing decarboxylated P1 arginine mimetics. *J. Med. Chem.* **2010**, *53*, 1067–1075.

(43) Shen, L.; Wang, F. W.; Cheng, A. B.; Yang, S. 2,2′-(Piperazine-1,4-diium-1,4-diyl)diacetate dihydrate. *Acta Crystallogr., Sect. E: Struct. Rep. Online* **2006**, *E62*, o2242–o2244.

(44) Ivanyi, T.; Lazar, I. Synthesis and in vitro enzyme hydrolysis of trioxadiaza- and tetraoxadiaza-crown ether-based complexing agents with disposable ester pendant arms. *Synthesis* **2005**, 3555–3564.

(45) Tanatani, A.; Mio, M. J.; Moore, J. S. Chain length-dependent affinity of helical foldamers for a rodlike guest. *J. Am. Chem. Soc.* **2001**, *123*, 1792–1793.

(46) Dietrich, W.; Nicklisch, S.; Koster, A.; Spannagl, M.; Giersiefen, H.; van de Locht, A. CU-2010–a novel small molecule protease inhibitor with antifibrinolytic and anticoagulant properties. *Anesthesiology* **2009**, *110*, 123–130.

(47) Mateescu, C.; Wikete, C.; Costisor, O.; Bouet, G.; Khan, M. A. Protonation behaviour of N,N′-piperazine-dipropionic acid. *C. R. Chim.* **2005**, *8*, 1149–1153.

(48) Ascenso, J. R.; Santos, M. A.; Frausto da Silva, J. J. R.; Vaz, M. C. T. A.; Drew, M. G. B. Protonation of diaza cyclic complexons: Proton NMR, calorimetric and molecular mechanics studies. *J. Chem. Soc., Perkin Trans. 2* **1990**, 2211–2218.

(49) Khalili, F.; Henni, A.; East, A. L. L. pK_a Values of Some Piperazines at (298, 303, 313, and 323) K. *J. Chem. Eng. Data* **2009**, *54*, 2914–2917.

(50) Marvin 5.11.4, 2012, ChemAxon (http://www.chemaxon.com)

(51) Figures 1 and 2 were created with the PyMOL Molecular Graphics System, version 1.2r2, Schrödinger, LLC.

(52) Lazar, H. L.; Bao, Y.; Tanzillo, L.; O'Gara, P.; Reardon, D.; Price, D.; Crowley, R.; Cabral, H. J. Aprotinin decreases ischemic damage during coronary revascularization. *J. Card. Surg.* **2005**, *20*, 519–523.

(53) Engles, L. Review and application of serine protease inhibition in coronary artery bypass graft surgery. *Am. J. Health-Syst. Pharm.* **2005**, *62*, S9–14.

(54) Saxena, P.; Thompson, P.; d'Udekem, Y.; Konstantinov, I. E. Kallikrein-kinin system: A surgical perspective in post-aprotinin era. *J. Surg. Res.* **2011**, *167*, 70–77.

(55) Westermann, D.; Schultheiss, H.-P.; Tschope, C. New perspective on the tissue kallikrein-kinin system in myocardial infarction: Role of angiogenesis and cardiac regeneration. *Int. Immunopharmacol.* **2008**, *8*, 148–154.

(56) Ruf, S.; Buning, C.; Schreuder, H.; Horstick, G.; Linz, W.; Olpp, T.; Pernerstorfer, J.; Hiss, K.; Kroll, K.; Kannt, A.; Kohlmann, M.; Linz, D.; Hubschle, T.; Rutten, H.; Wirth, K.; Schmidt, T.; Sadowski, T. Novel β-amino acid derivatives as inhibitors of cathepsin A. *J. Med. Chem.* **2012**, *55*, 7636–7649.

(57) Paju, A.; Stenman, U.-H. Biochemistry and clinical role of trypsinogens and pancreatic secretory trypsin inhibitor. *Crit. Rev. Clin. Lab. Sci.* **2006**, *43*, 103–142.

(58) Gustafsson, D.; Bylund, R.; Antonsson, T.; Nilsson, I.; Nyström, J. E.; Eriksson, U.; Bredberg, U.; Teger-Nilsson, A. C. A new oral anticoagulant: The 50-year challenge. *Nat. Rev. Drug Discovery* **2004**, *3*, 649–659.

(59) Gustafsson, D.; Antonsson, T.; Bylund, R.; Eriksson, U.; Gyzander, E.; Nilsson, I.; Elg, M.; Mattsson, C.; Deinum, J.; Pehrsson, S.; Karlsson, O.; Nilsson, A.; Sorensen, H. Effects of melagatran, a new low-molecular-weight thrombin inhibitor, on thrombin and fibrinolytic enzymes. *Thromb. Haemostasis* **1998**, *79*, 110–118.

(60) Dixon, M. The determination of enzyme inhibitor constants. *Biochem. J.* **1953**, *55*, 170–171.

(61) Stürzebecher, J.; Prasa, D.; Hauptmann, J.; Vieweg, H.; Wikström, P. Synthesis and structure-activity relationships of potent thrombin inhibitors: piperazides of 3-amidinophenylalanine. *J. Med. Chem.* **1997**, *40*, 3091–3099.

(62) LeadIT, version 2.0.2; BioSolveIT GmbH: Sankt Augustin, Germany.

(63) MOE, version 2010; Chemical Computing Group: Montreal, Canada.

(64) Labute, P. LowModeMD—Implicit low-mode velocity filtering applied to conformational search of macrocycles and protein loops. *J. Chem. Inf. Model.* **2010**, *50*, 792–800.